

Real-time Control of Neoclassical Tearing Mode in Time-dependent Simulations on KSTAR

Yong-Su Na 1), Kyungjin Kim 2), Hyunseok Kim 2), M. Maraschek 3), Y. S. Park 4), J. Stober 3), L. Terzolo 5), H. Zohm 3) and ASDEX Upgrade Team 3)

1) Department of Nuclear Engineering, Seoul National University, Seoul, Korea

2) Department of Energy System Engineering, Seoul National University, Seoul, Korea

3) Max-Planck-Institut für Plasmaphysik, Garching, Germany

4) Department of Applied Physics and Applied Mathematics, Columbia University, New York, USA

5) National Fusion Research Institute, Daejeon, Korea

e-mail contact of main author: ysna@snu.ac.kr

Abstract. As neoclassical tearing mode (NTM) sets a limit on achievable plasma beta, its control is one of major concerns in present and future tokamaks aiming at achieving high fusion performance. In this work, real-time feedback control of NTM by electron cyclotron current drive (ECCD) is simulated using a transport code, ASTRA, coupled with a solver of the modified Rutherford equation and an electron heating and current drive module. The plasma equilibrium, transport, heating and current drive, and the island evolution is calculated self-consistently. Firstly, the simulation tool is validated against experimental result in ASDEX Upgrade. Secondly, after the validation, the tool is adjusted to KSTAR specifications and a prediction of NTM activities is made in a KSTAR plasma. Thirdly, plasma response models describing relationship between the poloidal ECCD launcher angle and the island width are extracted by the system identification method. Lastly, a controller is designed based on the optimal response model and the performance of which is evaluated on KSTAR. Based on the results, performance of the NTM control is expected to be highly improved by optimising alignment between the island and the ECCD. This will strongly contribute to ITER as well as forthcoming KSTAR experiments.

1. Introduction

As the fusion era is rapidly approaching, the necessity of developing high performance steady state operation scenarios becomes more and more important, particularly for economically viable fusion power plants based on the tokamak concept. Neoclassical tearing mode (NTM), a type of resistive instability, is one of major concerns in present and future tokamaks aiming at achieving plasmas with such high fusion performance. It significantly degrades plasma confinement and angular momentum due to increase of the radial transport across the island region, consequently imposing a limit on plasma beta and even leading to plasma disruption. Therefore, a control of NTM is one of key issues in KSTAR and ITER targeting high-beta plasmas. Since the first observation of NTM in the TFTR experiment [1], a lot of progress has been made in recent years in physics and control technologies. It is verified experimentally that NTM is triggered by a perturbation of the bootstrap current due to the local flattening of the pressure profile over seed magnetic islands produced by MHD events, such as sawteeth. Based on theoretical analyses, the time evolution of NTM can be interpreted and predicted by the modified Rutherford equation (MRE) [2]. A variety of avoiding or controlling strategies are developed; reducing seed islands produced by other instabilities, using external helical fields to inhibit the perturbed bootstrap currents, applying radio frequency current drive (RFCD) accurately on the island [3], etc. Particularly, the method using localised current drive to replace the missing bootstrap current by electron cyclotron current drive (ECCD) is expected to be one of the most promising ways for active stabilisation of the NTMs due to its narrow deposition width and furthermore its equipment of the real-time steerable mirror in the engineering point of view. However, it is difficult to align ECCD to the location of the NTM

accurately because of variation of the ECCD deposition and the island location in time according to the evolution of the plasma equilibrium and transport. NTMs are usually triggered in rather dynamic phases where β_N is increasing and applying ECCD to suppress them brings additional perturbation to the plasma state. Moreover, a further increase of the heating power to increase β_N after the removal of the NTM can excite another NTM at higher β_N due to the changed plasma equilibrium and transport and the resulting misalignment of the ECCD with the resonance surface [4]. They address the requirement of the self-consistent analysis of the NTM evolution coupled with the plasma transport and equilibrium, particularly in view of closed-loop control.

In this work, real-time feedback control of NTM in KSTAR is simulated using a transport code, ASTRA [5], coupled with the MRE where the plasma equilibrium, transport and island evolution is calculated self-consistently. Firstly, a plasma model is set in ASTRA to describe the NTM evolution together with the plasma equilibrium and transport in a self-consistent way (section 2.1.). Secondly, the model is validated against experimental data from ASDEX Upgrade in section 2.2. Thirdly, the simulation tool is applied to KSTAR plasmas and a plasma response model is developed which describes the relationship between the ECCD angle and the island width in KSTAR (section 3.1 and 3.2). Fourthly, a dynamic feedback controller is developed based on the plasma response model by considering various time scales, i.e. plasma transport, the NTM growth rate, controller response. Then, lastly, closed-loop time-dependent simulations are executed and the performance of the real-time controller is evaluated in section 3.3.

2. Validation of the NTM Model against Experimental Results from ASDEX Upgrade

2.1. Description of modelling tools

The plasma transport code employed for this work is ASTRA [5] which solves coupled, time-dependent, 1-D transport equations for particles, heat, and current. The 2-D MHD fixed boundary equilibrium with a realistic tokamak geometry is solved by the ESC code [6] which is incorporated with ASTRA for self-consistent calculations. The neutral beam injection (NBI) package [7] is embedded in ASTRA for the calculation of NBI heating and CD. TORAY-GA [8] is coupled with ASTRA for ECRH/ECCD calculations. The Hirshman [9] model and the Sauter [10] model are used for plasma resistivity and for bootstrap current, respectively. The simulation prescribes Z_{eff} to 2.0 and includes Bremsstrahlung, cyclotron and line radiation from Carbon. A solver of MRE is coupled with ASTRA to calculate the time evolution of widths of islands self-consistently. The MRE implemented in ASTRA is as follows [11];

$$\frac{\tau_R}{r_s} \frac{d\omega}{dt} = \Delta'_0 r_s + \delta\Delta' r_s + a_2 \frac{j_{bs}}{j_{\parallel}} \frac{L_q}{\omega} \left[1 - \frac{\omega_{marg}^2}{3\omega^2} - K_1 \frac{j_{ec}}{j_{bs}} \right]$$

In the equation, all the variables are calculated by ASTRA. Among them, particularly the geometric constant a_2 is inferred from the saturated island width by ISLAND [12] that is also embedded in ASTRA for self-consistent calculations. Here, ion and electron temperature, electron density, and toroidal rotation profiles are taken from experiment for the simulation. The poloidal rotation is assumed to be neoclassical [13].

2.2. Validation of the Model against the NTM Control Experiment in ASDEX Upgrade

As a new ECRH system was designed in ASDEX Upgrade recently, delicate control of the NTM activities are possible using a fast movable launcher which can move with a speed of 10 degrees in 100 ms. Taking acceleration phases into account it takes for example ~ 30 ms to move by 2 degrees which is small with respect to the NTM growth rate of ~ 100 ms. Figure 1 (a) represents one of the feed-forward (3,2) NTM stabilisation experiments performed in ASDEX Upgrade (pulse 25845) [14-16]. Plasma current is 1 MA and toroidal magnetic field is 2.52 T. NBI power of 10 MW is applied to raise β_N high enough to trigger the (3,2) NTM in an H-mode plasma. At 1.5 s, off-axis ECCD is modulated with a frequency of 250 Hz at 1 MW power combined with central ECRH of 1 MW power but without modulation. The off-axis ECCD profile is adjusted to be located accurately relative to the position of the respective NTM by steering the launcher iteratively to the coincidence position. The variation of the launcher angle and corresponding response of the amplitude of the (3,2) NTM is presented in figure 1 (a). After stabilisation of the (3,2) NTM, β_N is observed to rise slightly.

The model introduced in section 2.1 is employed to reproduce the experiment. The simulation starts at 0.98 s and a seed island is forced to appear at 1.7 s with 0.016 m of width. As shown in figure 1 (b), the time evolution of the island width simulated by the model is in good agreement with the experiment prior to 3.3 s. The trend of the island width variation according to the scan of the poloidal launching angle is also reproduced by the simulation. For some reasons, the island is grown instantly around 3.3 s as indicated by spikes in the figure during the experiment. The simulation overemphasises this behaviour occurring at 3.3 s so that the island is not suppressed but survived for a longer time than the experiment. It is noteworthy that the simulation is highly sensitive to selection of the initial q -profile since by which parameters such as L_q and j_{\parallel} in MRE as well as the island location are determined. Since MSE data is not available in this pulse, the initial q -profile is estimated from equilibrium reconstruction using magnetic diagnostics for this simulation.

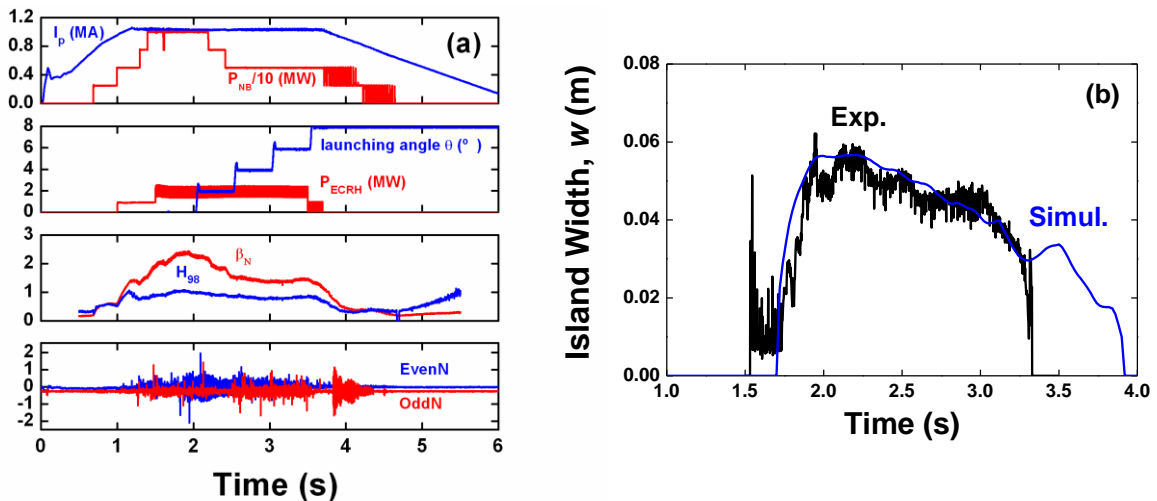


FIG. 1. (a) Overview of a feed-forward (3,2) NTM stabilisation experiment in ASDEX Upgrade (Pulse 25845) (b) Comparison of time evolution of the (3,2) island width between the experiment and the simulation

3. Simulation of Real-time Feedback Control of NTM in KSTAR

3.1. Modelling of NTM Control in KSTAR

The same plasma model is set in ASTRA to predict the NTM evolution coupled with the plasma equilibrium and transport in a self-consistent way at KSTAR. However, as no

experimental data is yet available in KSTAR, the Weiland transport model [17] is employed for calculating anomalous heat transport to predict temperature profiles. The Weiland model is a fluid model based on ion temperature gradient (ITG) and trapped electron mode (TEM) which predicts thresholds in both ion and electron temperature gradient lengths; if the gradients are below the critical value, transport is neoclassical. The neoclassical ion and electron transport coefficients are taken from [18] and [19], respectively. The heat diffusivities inside islands are manipulated to increase enough to flatten temperature profiles as shown in figure 2 (a) so that effects of NTM to the plasma transport are considered; $\chi_i = \chi_e = 40$ inside the islands, otherwise, $\chi_{i,e} = \chi_{i,e}^{NC} + \chi_{i,e}^{GLF}$. The boundary conditions of the ion and electron temperature are given at $\rho_{tor} = 0.8$ taken from the experiment shown in section 2.2. Perturbation in the bootstrap current due to the flattening of temperature profiles results in local reduction of total current density as shown in figure 2 (c). However, no flattening is forced in density profiles. Here, the particle transport is not solved but experimental density profile is used taken from the experiment. The plasma current and the magnetic field are set to the same values as pulse 25845; 1 MA and 2.52 T, respectively. The simulation starts at 1.0 s. NBI power of 8.1 MW is applied from three beam sources which increases β_N up to ~ 2.6 , high enough to trigger the (3,2) NTM.

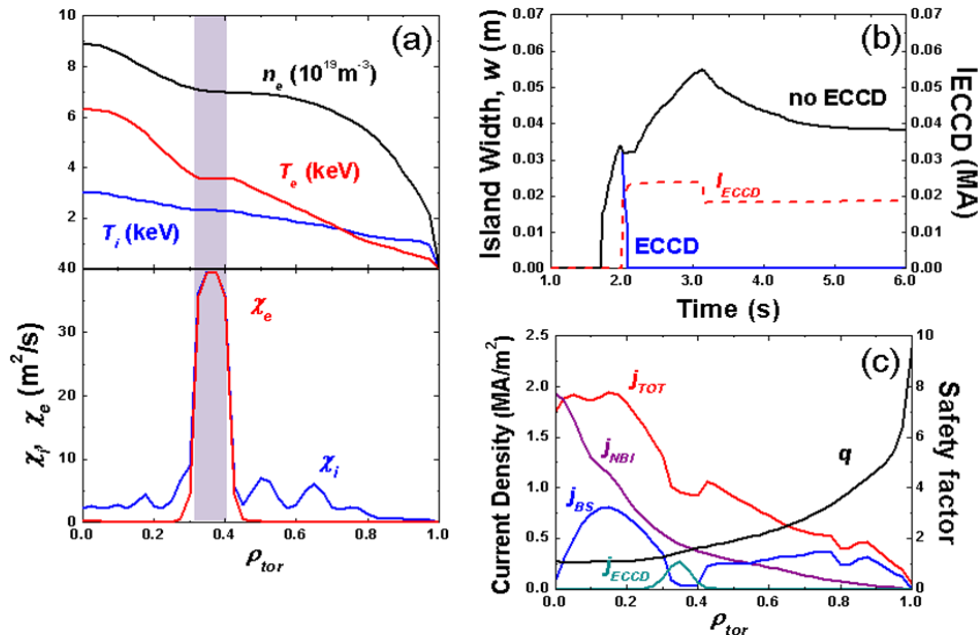


FIG. 2. Flattening of temperature profiles at the (3,2) island location due to deliberate increase of heat diffusivities (a), time evolutions of ECCD current and the island width with and without ECCD (b), total, NBI driven, EC driven, bootstrap current density and q profile (c) at around 2.0 s in the NTM simulation of KSTAR.

The time trace of the island width is shown in figure 2 (b). The initial width of the seed island to initiate the (3,2) NTM is postulated to be 1.5 cm at 1.7 s inferred by ISLAND. As shown in the figure, the (3,2) mode grows up to 0.055 m, then decreases and saturates around 0.038 m.

The effect of ECCD is investigated by applying ECRH with power of 1 MW at 170 GHz X2 mode at 2.0 s without modulation. The launcher is located at $R = 2.785$ m, $Z = -0.14$ m and the poloidal and the toroidal angle are 90° and 190° , respectively. The (3,2) mode is stabilised quickly after applying ECCD in about 100 ms as represented by blue solid curve in figure 2 (b); ECCD is applied at 2.0 s and the island is suppressed around 2.08 s. The EC

launcher angle is selected to drive current at the O-point of the island to compensate the loss of bootstrap current as clearly seen in figure 2 (c).

3.2. System Identification

A plasma response model is developed which describes the relationship between the ECCD angle and the island width in KSTAR. The toroidal angle (φ) of 190° and poloidal angle (θ) of 90° is used as reference values to derive the plasma response model since they are evaluated as the optimal angle of the ECCD launcher at B_{tor} of 2.52 T to stabilise the (3,2) NTM, provided that the plasma is in a stationary condition. For system modelling, it is possible to choose the input parameter as the ECCD launch angles (poloidal or toroidal) and ECH power. Among them, the poloidal launch angle is defined as the input parameter in this paper by considering that the ECCD launcher usually cannot change the poloidal and the toroidal angle simultaneously during a discharge. The island width is selected as output parameter. For system identification, the modulation of the input parameter is needed to catch the behaviour of the output parameter. Various time scales including heat transport, current diffusion and actuator response are considered to determine a frequency spectrum of a pseudobinary noise modulation [20]. The pseudobinary noise modulation is a rectangular waveform with modulated pulse width and has a frequency spectrum similar to that of a continuous noise signal. The pseudobinary noise modulation signal can be decomposed into a spectrum of discrete frequencies: $f_k = K/2Nl\Delta t$, where N is the order of the pseudobinary noise, Δt sampling time, and l the minimum pulse length of the modulation signal in units of sampling time [20]. The usable frequency range lies between $0 < f_k < 2/\Delta t$ (Nyquist criterion). This frequency range covers all principal dynamic properties of the system to be identified by considering the various time scales in the plasma. The waveform of the modulation is shown in figure 3 (a). Here, Δ is defined as the difference between modulated and reference (not-modulated) values. The case without ECCD presented in figure 2 is chosen as the reference for the system identification.

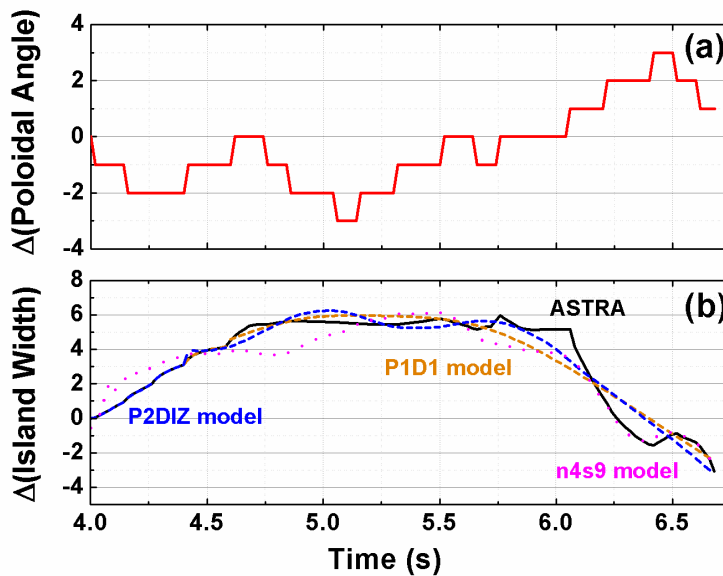


FIG. 3. Waveform of the modulated ECH poloidal launch angle respect to the reference one (a), variation of the island width respect to the reference one according to the modulation of the poloidal angle calculated by two process models (P2DIZ, P1D1) and one linear state-space model (n4s9) (b). Here, the ASTRA simulation is presented as the black curve.

In the simulation with the modulated poloidal angle, ECCD is applied and modulated at 4.0 s where the plasma approaches stationary conditions. The initial poloidal and toroidal angles are the same as those in section 3.1, 90° and 190° , respectively. The island width begins to decrease as soon as a localised current driven by ECCD is deposited at the island location. On the contrary, if the current is driven at the wrong position due to change of the angle, the island starts growing, that is represented as positive values of $\Delta(\text{Island Width})$ before 6.25 s in the black solid curve (see figure 3 (b)). The modulated ASTRA simulation together with the reference without ECCD is used to build plasma response models which can extract the relationship between the angle and the island width. A linear state-space model (n4s9) and two process models (P2DIZ, P1D1) are employed. As shown in figure 3, the P2DIZ, the P1D1, and the n4s9 model exhibit fit accuracies of about 77.24%, 73.51%, and 65.98 %, respectively as shown in figure 3 (b), where the fit accuracy of the model is defined as follows;

$$\text{Fit accuracy (\%)} = \left[1 - \frac{|y - \hat{y}|}{|y - \bar{y}|} \right] \times 100$$

where y is the measured/reference output from ASTRA simulations and \hat{y} is simulated/predicted output from each model, and \bar{y} is the mean value of y .

To validate the system models established, the database with another modulation form is produced by a NTM simulation using ASTRA. The minimum time step of the modulation is 100 ms and the time duration is set to be different each other as shown in figure 4 (a). The models are tested to reproduce the behaviour of the island width according to the given modulation form of the poloidal angle. As a result, the P2DIZ, the P1D1, and the n4s9 model exhibit fit accuracies of about 88.74%, 97.98%, and -31.66 %, respectively as shown figure 4 (b). A negative value of fit accuracy implies that the model is no better than guessing the output to be a constant ($\hat{y} = \bar{y}$) by definition. The process models fit the reference successfully, however the linear model fails to reproduce it. The P1D1 model exhibiting the best performance at validation is chosen to design a controller in the next section.

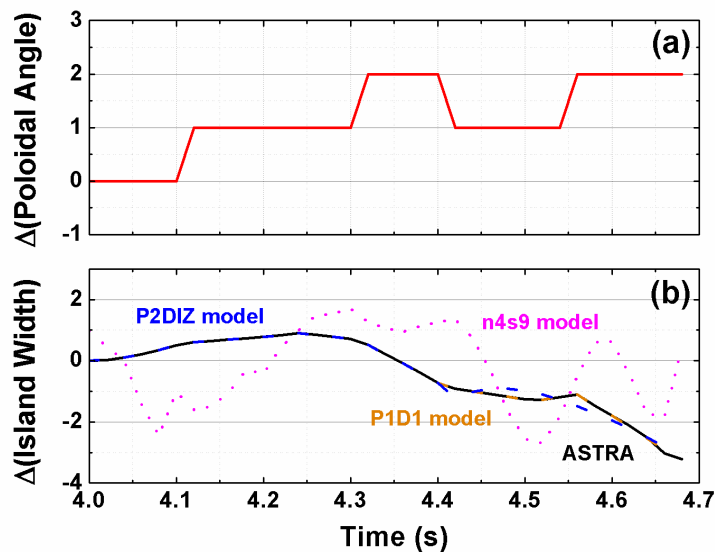


FIG. 4. Waveform of the modulated ECH poloidal launch angle respect to the reference one for evaluating the models (a), variation of the island width respect to the reference one according to the modulation of the poloidal angle calculated by two process models (P2DIZ, P1D1) and one linear state-space model (n4s9) (b). Here, the ASTRA simulation is presented as the black curve.

3.3. Simulation of Real-time Feedback Control of NTM

A proportional-integral-derivative (PID) controller is developed for a dynamic feedback control of (3,2) NTM based on the PID1 model. The controller attempts to search and suppress the island by changing the poloidal launch angle. For the best performance, the PID parameters must be tuned according to the characteristic of the system. They are determined as $K_p = 2$, $K_i = 0.15$ and $K_d = 3.05$ in the feedback control simulation for KSTAR.

Closed-loop time-dependent simulations are executed and the performance of the real-time controller is evaluated. The plasma conditions except the starting time of ECCD are same as the scenario introduced in section 3.1. The ECCD is applied at 2.85 s when the island width is grown as large enough. The initial launch angle, the toroidal angle of 190° and poloidal angle of 90° evaluated as optimal value if applied at 2.0 s, is no longer most favourable to suppress NTM at 2.85 s because the plasma transport and equilibrium is varied after 2.0 s so that the island location and the ECCD deposition are not necessarily aligned. For this reason, the island width is growing after injection of the ECCD as shown in the blue curve in figure 5 (a) even larger than that in the case of without ECCD, presented as black curve in figure 5 (a). One can easily deduce that the ECCD deposition is definitely misaligned to the island at this time point. However, as the simulation goes on the plasma evolves to match the ECCD deposition to the island resulting in suppression of the mode around 5.4 s as shown in figure 5 (a). If the PID controller is turned on in the same condition, the controller tries to adjust the poloidal angle about 0.2° per 20 ms in order to deposit the ECCD on the exact location of the island in real-time (see the red curve in figure 5 (a)). As a result, the island is completely suppressed in 300 ms which makes a considerable contrast to the case without feedback control which requires about 2.56 s to suppress the NTM completely. Although the island width is increased in the initial phase after the ECCD is applied compared with the case with no ECCD (black curve in figure 5 (a)), the controller turns the direction in a short time period. Therefore, it is expected that the controller is able to handle the initial misalignment of the ECCD to the island.

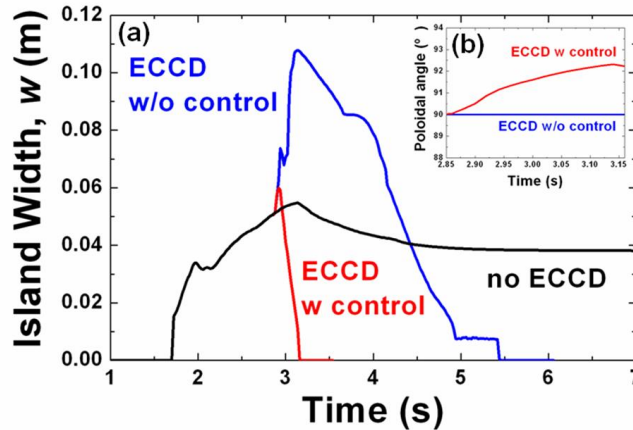


FIG. 5. Time evolutions of the island width with and without ECCD to evaluate the performance of the real-time controller (a), time variation of the poloidal angle with and without controller during the feedback control time from 2.85 s to 3.15 s (b)

4. Summary and Conclusions

Real-time feedback control of NTM by ECCD is simulated using a transport code, ASTRA, coupled with a solver of the MRE and TORAY-GA for ECH&CD calculations. The plasma

equilibrium, transport, heating and current drive, and the island evolution is calculated self-consistently. Firstly, the simulation tool is validated against experimental result in ASDEX Upgrade. The time trend of the island width according to the variation of the poloidal ECCD launcher angle is mostly reproduced except the very last moment. Secondly, the simulation tool is applied to KSTAR to predict (3,2) NTM activities. Heat diffusivities are calculated by the Weiland model for the outside region of the island and they are manipulated to flatten temperature profiles inside the island. Thirdly, plasma response models describing relationship between the poloidal ECCD launcher angle as the input parameter and the island width as the output parameter are identified by the system identification method. A pseudobinary noise modulation is forced to the poloidal launch angle and the response of the island width is saved as database to extract models. Three models, one linear and two process models, are established and evaluated using another database containing a different waveform of the modulation. The process models are observed to exhibit higher accuracies in reproducing the reference data compared with the linear one. Lastly, a controller is designed based on the optimal response model and the performance of which is evaluated. It is shown that the controller searches the position of the island and suppresses it successfully although the initial launcher angle is aligned badly to the island. Based on the results, performance of the NTM control is expected to be highly improved in the experiments that will strongly contribute to ITER as well as forthcoming KSTAR experiments.

Acknowledgements

This work was supported by Basic Science Research Program through the National Research Foundation of Korea (NRF) funded by the Ministry of Education, Science and Technology (MEST) (NRF-2010-0001841).

References

- [1] Chang Z *et al* 1995 *Phys. Rev. Lett.* **74** 4663
- [2] Sauter O *et al* 1997 *Phys. Plasmas* **4** 1654
- [3] Zohm H. *et al* 1999 *Nucl. Fusion* **39** 577
- [4] Maraschek M *et al* 2005 *Nucl. Fusion* **45** 1369
- [5] Pereverzev G *et al* 2002 IPP-Report IPP 5/98
- [6] Zakharov L E *et al* 1999 *Phys. Plasmas* **6** 4693
- [7] Polevoi A *et al* 1997 JAERI-Data/Code 97-014
- [8] Kritz A H *et al* Heating in Toroidal Plasmas 1982, in *Proceedings of the 3rd Joint Varenna-Grenoble Int. Symp. Grenoble, Brussels, 1982, Vol. 2 CEC, p. 707*
- [9] Hirshman S P *et al* 1977 *Nucl. Fusion* **17** 611
- [10] Sauter O *et al* 1999 *Phys. Plasmas* **6** 2834
- [11] Park Y S *et al* 2008 *Journal of Korean Phys. Society* **53** 1923
- [12] Nguyen C N, Bateman G and Kritz A H 2004 *Phys. Plasmas* **11** 3460
- [13] Staebler G M *et al* 1997 *Nucl. Fusion* **37** 287
- [14] Reich M *et al* 2010 *Proc. 37th European Physical Society Conf. on Controlled Fusion and Plasma Physics (Dublin, Ireland, 2010)* P2.189
- [15] Reich M *et al* 2010 *accepted in Fusion Science and Technology*
- [16] Stober J *et al* 2010 *Proc. 16th Joint Workshop on Electron Cyclotron Emission and Electron Cyclotron Resonance Heating (Sanya, China, 2010)*
- [17] Weiland J *et al* 1989 *Nucl. Fusion* **29** 1810
- [18] Galeev A A and Sagdeev R Z 1973 *Voprosy Teorii Plasmy* **7** 210
- [19] Angioni C and Sauter O 2000 *Phys. Plasmas* **7** 1224
- [20] Godfrey K "Perturbation Signals for System Identification" 1993 Prentice-Hall, Englewood Cliffs, New Jersey